IOPscience iopscience.iop.org

Home Search Collections Journals About Contact us My IOPscience

Effective-mass anisotropy in GaAs-(Ga,Al)As two-dimensional hole systems: comparison of theory and very high-field cyclotron resonance experiments

This article has been downloaded from IOPscience. Please scroll down to see the full text article.

1995 J. Phys.: Condens. Matter 7 L675

(http://iopscience.iop.org/0953-8984/7/48/003)

View the table of contents for this issue, or go to the journal homepage for more

Download details:
IP Address: 171.66.16.151
The article was downloaded on 12/05/2010 at 22:34

Please note that terms and conditions apply.

J. Phys.: Condens. Matter 7 (1995) L675–L681. Printed in the UK

LETTER TO THE EDITOR

Effective-mass anisotropy in GaAs–(Ga, Al)As two-dimensional hole systems: comparison of theory and very high-field cyclotron resonance experiments

B E Cole†, W Batty‡, Y Imanaka§, Y Shimamoto§, J Singleton‖, J M Chamberlain†, N Miura§, M Henini† and T Cheng†

† Department of Physics, The University of Nottingham, Nottingham NG7 2RD, UK
‡ Electronics Department, The University of York, Heslington, York YO1 5DD, UK
§ Institute for Solid State Physics, The University of Tokyo, Minato-ku, Tokyo 106, Japan
‖ Department of Physics, University of Oxford, Clarendon Laboratory, Oxford OX1 3PU, UK

Received 25 July 1995, in final form 2 October 1995

Abstract. Cyclotron resonance of two-dimensional holes in high-mobility GaAs–(Ga, Al)As heterojunctions with the growth directions [011], [111], [211], [311] and [100] has been measured at magnetic fields of around 35 T, corresponding to Landau level occupancies deep in the ultraquantum limit. A manipulation of the standard four-band Luttinger Hamiltonian has been used to show that the behaviour of the hole ground state is dominated by the leading field-dependent term in a power series expansion for the Landau level dispersion. The experimentally observed trend in measured effective mass with substrate orientation can therefore be qualitatively explained in terms of the variation of bulk hole mass with crystallographic direction.

The subband structure of two-dimensional electron systems in GaAs–(Ga, Al)As heterostructures is relatively straightforward and for many applications, such as the design of simple devices, may be approximated by parabolic, isotropic subbands. For the equivalent hole systems, on the other hand, no such simplifications may be made, and in order to design devices involving holes in a predictable way, knowledge of the detail of the hole subbands is essential. The hole subband structure realized in a heterostructure depends critically on the orientation of the substrate and the width of the confinement potential [1, 2] and this letter reports a study of the dependence of hole subband structure on substrate orientation (i.e. growth axis). The standard four-band Luttinger Hamiltonian [3] has been manipulated to provide a 'rotated' valence band Hamiltonian which can be used to derive hole subband structure and Landau level dispersion relations for heterostructures with generic growth axes [*hkk*], where h and k are integers. The results are compared with cyclotron resonance measurements of the hole effective mass in high-mobility GaAs–(Ga, Al)As heterojunctions with the growth directions [011], [111], [211], [311] and [100] carried out at magnetic fields of around 35 T. A power series expansion for the hole Landau level dispersion shows that the behaviour of the hole ground state is largely determined by the three-dimensional topology of the bulk hole bands and that, despite the known complexity of hole Landau level structure [4, 5], the experimentally observed trend in cyclotron resonance masses can be qualitatively explained in terms of the variation of bulk hole mass with crystallographic direction.

0953-8984/95/480675+07$19.50 © 1995 IOP Publishing Ltd

Table 1. Sample growth orientations, areal hole densities p_s, low-temperature mobilities μ and cyclotron resonance (CR) effective masses measured at 10.5 meV. The effective masses are averaged values and are accurate to $\pm 0.005\ m_e$.

Growth plane	(100)	(311)B	(211)B	(111)B	(011)
p_s (10^{11} cm^{-2})	2.8	2.5	3.9	3.2	1.8
μ (m^2 V^{-1} s^{-1})	12	5.6	1.45	3.8	7.2
CR mass (m_e)	0.395	0.388	0.355	0.335	0.359

The GaAs–(Ga, Al)As heterojunctions were grown under similar conditions on the crystal planes (100), (311)B, (211)B, (111)B and (011) by molecular beam epitaxy [6]. Samples from this series had the following layer structure: semi-insulating substrate, 1 μm undoped GaAs, 50-period GaAs–AlAs superlattice, 0.5 μm undoped GaAs, 50 nm undoped $Ga_{0.67}Al_{0.33}As$ spacer layer, 40 nm $Ga_{0.67}Al_{0.33}As$ doped with 1×10^{18} cm^{-3} of Be, 17 nm GaAs capping layer. Areal hole densities p_s and low-temperature mobilities μ for the samples are given in table 1. Note that the sample substrates were wedged to avoid distortion of the cyclotron resonance (CR) lineshape due to interference [7]. The CR was measured using direct absorption of monochromatic far-infrared radiation from a gas-discharge molecular (H_2O) laser (wavelength $\lambda = 118.5910$ μm, photon energy $h\nu_L \approx 10.5$ meV [8]). The samples were cooled with flowing He gas, enabling their temperature to be maintained at 16 K. Pulsed magnetic fields of up to $B \sim 80$ T were generated using the single-turn coil technique [9]. The reasons for using high fields were fourfold.

(i) The areal carrier density varies from sample to sample, so the confining potentials are not identical amongst the samples. Hence, a meaningful comparison of samples should minimize the contribution of the confinement energy to the observed effective mass. This is accomplished by maximizing the cyclotron energy, i.e. by using as large a magnetic field as possible.

(ii) At $h\nu_L \approx 10.5$ meV, the CRs for all the samples occur at between 30 and 35 T—more than twice the field at which the Fermi energy drops into the lowest Landau state even in the sample with the highest carrier density (the number of filled Landau states is $\nu = hp_s/eB$). This ensures that the initial and final Landau states involved in the CR are the same in all samples.

(iii) The high fields ensure that the CR linewidth is narrow, so the resonance position can be accurately located.

(iv) The recently observed phenomenon of correlated cyclotron resonance can result in a temperature-dependent shift of the CR position [10, 11], which could cause a small error if the samples were examined at inconsistent temperatures. This effect is minimized by using as high a field as possible.

Figure 1 shows examples of typical experimental magnetotransmission data at $h\nu_L \approx 10.5$ meV for all of the samples. The CR are observed as dips in the transmission centred on the resonance field B_{res} [7]. The observed CR effective masses are given by $eB_{res}/h\nu_L$; averaged values (from a number of field sweeps) are shown in table 1.

A limited number of CR experiments were also performed using the $\lambda = 163.033\,53$ μm ($h\nu_L \approx 7.6$ meV) line [8] of an optically pumped molecular gas (CH_3OH) laser; the effective masses derived were found to follow a similar trend with substrate orientation [11] to that of the $h\nu_L \approx 10.5$ meV data.

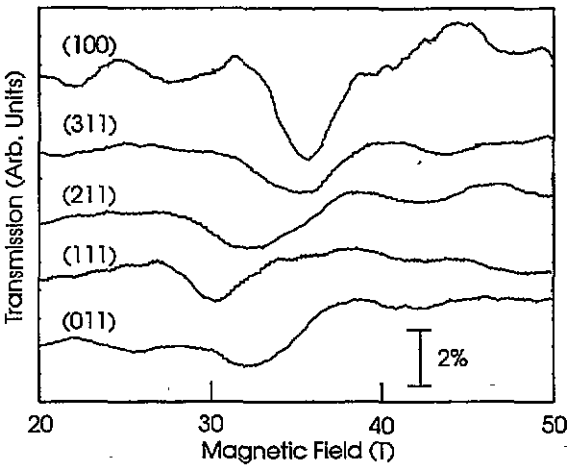

Figure 1. Typical examples of magnetotransmission data for all five samples obtained using the 10.5 meV laser line. The temperature is ≈16 K.

The valence band structure of bulk (Ga, Al)As is accurately described by the four-band Luttinger Hamiltonian [3] and heterostructure valence subband dispersion can be derived from the bulk Hamiltonian in the envelope function approximation [12]. The effects of an external magnetic field are readily included by substitution of simple harmonic oscillator raising and lowering operators for the in-plane wavevector components in the coupled envelope function equations [13].

The standard form of the bulk Luttinger Hamiltonian has x, y, z along crystallographic $\langle 100 \rangle$ directions, and making the substitution $k_z \rightarrow -\mathrm{i}\,\mathrm{d}/\mathrm{d}z$, for bulk wavevector k_z parallel to the heterostructure growth axis, corresponds to growth on a {100} plane. By a rotation of axes, the bulk Hamiltonian can be expressed in terms of x', y', z' coordinates along non-$\langle 100 \rangle$ directions and $k_{z'} \rightarrow -\mathrm{i}\,\mathrm{d}/\mathrm{d}z'$ then describes heterostructure growth on a non-{100} plane.

Equation (1) gives the diagonal terms $a_{\pm}$ of the rotated Luttinger Hamiltonian for z' along $[l11]$, x' along $[2\bar{l}\bar{l}]$ and y' along $[01\bar{1}]$:

$$a_{\pm} = \frac{\hbar^2}{m_e}\frac{1}{2}\left[\gamma_1 \mp 2\sqrt{\xi^2\gamma_2^2 + (1-\xi^2)\gamma_3^2}\right]k_{z'}^2 + \frac{\hbar^2}{m_e}\frac{1}{2}\left[\gamma_1 \pm \frac{\xi\gamma_2^2 + (1-\xi)\gamma_3^2}{\sqrt{\xi^2\gamma_2^2 + (1-\xi^2)\gamma_3^2}}\right]k_{\rho'}^2$$
$$\pm \frac{\hbar^2}{m_e}\frac{\xi(1-\xi)}{\sqrt{\xi^2\gamma_2^2 + (1-\xi^2)\gamma_3^2}}(\gamma_3^2 - \gamma_2^2)(\cos^2\phi' k_{\rho'}^2 + \sqrt{2}l\cos\phi' k_{\rho'}k_{z'}). \qquad (1)$$

with

$$\xi = \frac{l^2 - 1}{l^2 + 2}.$$

Here, $(k_{\rho'}, \phi')$ are the polar coordinates of the bulk wavevector in the $k_{x'}k_{y'}$-plane. With the replacement $k_{z'} \rightarrow -\mathrm{i}\,\mathrm{d}/\mathrm{d}z'$ the Hamiltonian is appropriate for heterostructures grown along an arbitrary $[hkk]$ axis, where $l = h/k$ is allowed to take non-integer values [14].

Key features of in-plane subband dispersion and of Landau level structure, for arbitrarily shaped quantum wells [16], can be inferred immediately from equation (1) using the general

relation $\gamma_1 > 2\gamma_3 > 2\gamma_2$ for the position-dependent Luttinger parameters; salient points are summarized below.

(i) The first term in $a_\pm$ is of the form

$$-\frac{\hbar^2}{m_e}\frac{1}{2}\frac{\mathrm{d}}{\mathrm{d}z'}\frac{1}{m_\parallel^{*\pm}(z')}\frac{\mathrm{d}}{\mathrm{d}z'},$$

where $m_\parallel^{*\pm}(z')$ is the bulk hole mass parallel to the QW growth direction. It determines the zone-centre (zero-field) subband energies for heavy (+) and light (−) holes. It is apparent, for instance, that for a given potential profile, zone-centre energies will be exactly the same for [011] as for [211] growth. The zone-centre subband separations (along with zone-centre envelope function overlaps) determine the mixing of the heavy- and light-hole states away from the zone centre and at finite fields, and therefore determine the corresponding zone-centre mass, degree of subband non-parabolicity and degree of Landau level non-linearity.

(ii) The second term in $a_\pm$ gives the bulk hole mass perpendicular to the quantum well growth axis $m_\perp^{*\pm}(z')$. The zone-centre quantum well effective mass of the nth heavy- or light-hole ($\alpha = \pm$) subband can be expressed in terms of this bulk in-plane mass in the exact form [17]

$$\frac{1}{m_{QWn}^{*\alpha}} = \int_{QW} |F_n^\alpha|^2 \frac{1}{m_\perp^{*\alpha}(z')}\,\mathrm{d}z' + 2\frac{\hbar^2}{m_e}\sum_{m\beta\neq n\alpha}\left|\int_{QW} F_n^{\alpha *}\left(\gamma\frac{\mathrm{d}}{\mathrm{d}z'}\right)_{herm} F_m^\beta\,\mathrm{d}z'\right|^2 \Big/ (E_n^\alpha - E_m^\beta) \tag{2}$$

where the E_n^α are zone-centre subband energies and the F_n^α are corresponding zone-centre envelope functions. This is the value to which, in the axial approximation, all $\Delta N = \pm 1$ cyclotron resonance masses tend in the limit $B \to 0$. Equation (2) states that the (inverse) zone-centre quantum well effective mass, for a given subband, is just the sum of the (inverse) bulk, position-dependent, in-plane mass, weighted by the corresponding envelope function (with integration over the quantum well from $-\infty$ to $+\infty$) plus a term (shown schematically) due to the mixing of zone-centre wavefunctions by the linear $k_{\rho'}$-terms of the bulk Luttinger Hamiltonian (with summation over all other zone-centre subbands for which the matrix elements are not identically zero).

The dominant term in equation (2) comes from the bulk in-plane mass, with subband mixing acting to increase the in-plane mass of the lowest-lying quantum well subband. Therefore, as the heterostructure growth axis varies, the general behaviour of the ground-state, zone-centre, quantum well hole subband mass (and so also of the axial approximation, $\Delta N = \pm 1$, $B \to 0$, cyclotron resonance mass) is expected to reflect the dependence of the bulk in-plane mass on crystallographic direction as described by the l-dependence of the second term in $a_\pm$.

(iii) The third term in $a_\pm$ describes the in-plane anisotropy of the bulk bandstructure in the diagonal approximation, i.e. ignoring off-diagonal terms of the Luttinger Hamiltonian. This term is seen to be zero for [100] and [111] growth. For other growth directions, the $k_{\rho'}^2$-term contributes to in-plane anisotropy of the zone-centre QW subband mass. The term linear in $k_{\rho'}$ is also zero for [011] growth, but for other growth directions can produce an additional, anisotropic contribution to the QW subband mass via subband mixing. The hermiticity of the envelope function Hamiltonian means that the subband dispersion still does not exhibit any linear dependence on $k_{\rho'}$.

To make direct comparison between theory and the experimentally observed cyclotron resonance masses, the bulk in-plane mass is averaged over in-plane angle ϕ'. This averaged

bulk in-plane mass is given by $m^{*\pm}_{\perp av} = (\hbar^2/m_e)(1/2\pi)\ \mathrm{d}A/\mathrm{d}E$, where A is the area in the $k_{x'}k_{y'}$-plane enclosed by a contour of constant energy E, and is simply evaluated analytically in terms of the coefficients of $k^2_{\rho'}$ in equation (1). This allows an effective axial approximation to be derived for the diagonal terms of the rotated Luttinger Hamiltonian:

$$a_{\pm} = \frac{\hbar^2}{m_e}\frac{1}{2}\frac{1}{m^{*\pm}_{\parallel}}k^2_{z'} + \frac{\hbar^2}{m_e}\frac{1}{2}\frac{1}{m^{*\pm}_{\perp av}}k^2_{\rho'}. \tag{3}$$

To obtain the effective mass measured at the Fermi level, well below the valence subband edge, the $N = 1$ and $N = 2$ heavy-hole Landau level dispersions [13] can then be expressed as power series expansions in magnetic field B:

$$\epsilon^{+}_{nN} = E^{+}_{n} + \int_{QW} |F^{+}_{n}|^2 \left[(2N-1)\frac{1}{m^{*+}_{\perp av}(z')} + \mu^{+}(l)\kappa(z')\right] \mathrm{d}z' \left(\frac{e\hbar}{2}\right) B + \sum_{m=2}^{\infty} c^{+}_{nN}(l) B^{m/2} \tag{4}$$

with the coefficient μ^{+} of the κ-terms being dependent on growth axis $[l11]$ [14]. The field-dependent cyclotron resonance mass for the ground-state, heavy-hole, $N = 1$ to $N = 2$, Landau level transition, given by $e\hbar B/(\epsilon^{+}_{nN\pm1} - \epsilon^{+}_{nN})$, is then seen to be of the form

$$m^{*+}_{CR}(B) = \frac{1}{(1/m^{*+}_{\perp av}) - \eta(B)} \tag{5}$$

where, in general, η is dependent on l and B and acts to increase the in-plane mass from its bulk, $B = 0$ value.

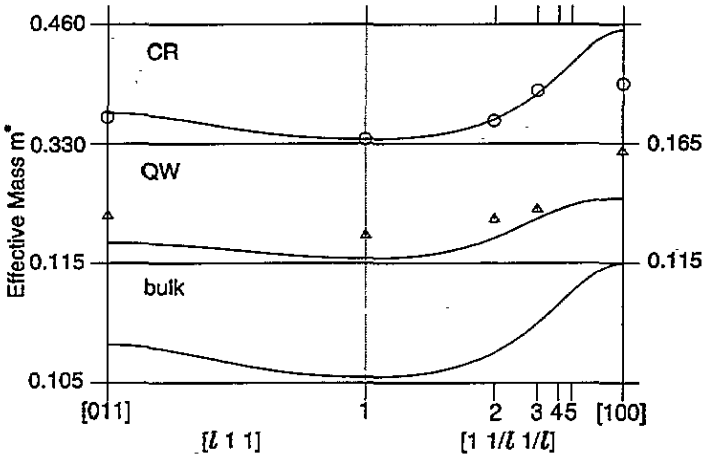

Figure 2. The variation of theoretical and experimental hole masses with growth direction $[l11]$. The bottom section shows the calculated bulk, in-plane-averaged, heavy-hole mass for GaAs, $m^{*+}_{\perp av}$. The middle section compares the calculated, in-plane-averaged, zone-centre mass for the ground-state heavy-hole subband in a square, 100 Å GaAs–(Ga, Al)As quantum well (triangles; after [19]) against an analytical expression for in-plane-averaged, zone-centre mass in an $[l11]$-grown, infinite square well (solid line). The uppermost section compares the experimental cyclotron resonance masses (circles), measured at $h\nu_L \approx 10.5$ meV, against mass m^{*+}_{CR} calculated assuming η constant and retaining only the l-dependence of the leading (bulk) field-dependent term in the power series expansion for Landau level dispersion (solid line).

Figure 2, bottom panel, illustrates how the bulk, in-plane-averaged, heavy-hole mass for GaAs, $m^{*+}_{\perp av}$, varies with crystallographic direction $[l11]$ as l varies between 0 and ∞,

i.e. as $[l11]$ varies from [011] to [11$\bar{1}$] and [1 $1/l$ $1/l$] varies from [111] to [100] (using $\gamma_1 = 6.78$, $\gamma_2 = 1.92$, $\gamma_3 = 2.70$ [18]). Figure 2, centre panel, compares values of the in-plane-averaged, zone-centre mass for the ground-state, heavy-hole subband in a square 100 Å GaAs–(Ga, Al)As quantum well, obtained from full quantum well subband structure calculations [19] (triangles), against the in-plane-averaged, zone-centre, subband mass from equation (2) evaluated explicitly for an infinite square well [17, 20] using the full $[l11]$ Hamiltonian [21] and GaAs parameters [18] (solid line). The analytical expression (with no free parameters) reproduces the trend in the numerically obtained masses and, despite the infinite-well approximation, gives quantitative agreement to better than 15% for all l.

The calculated bulk in-plane mass implicitly assumes negligible wavefunction penetration into the barriers and neglects all quantum well subband mixing. The quantitative differences between the 100 Å quantum well, zone-centre mass and the bulk mass can therefore be understood in terms of the position dependence of the bulk in-plane mass in the finite well and the subband mixing contribution to the quantum well mass, as illustrated by equation (2). These factors alter the values of calculated in-plane mass, but only serve to accentuate the underlying trend resulting from the l-dependence of the bulk mass.

Figure 2, top panel, compares the experimentally obtained cyclotron resonance masses (circles) against the mass m^{*+}_{CR} calculated from equation (5), with η assumed independent of l and B and chosen to exactly reproduce the value of the experimental [111] mass (solid line). Agreement to ~1% is obtained for the [011], [111] (by definition of η), [211] and [311] masses, with only one free parameter, η, and the [100] mass is also seen to follow the calculated trend, though it does not lie on the analytically obtained curve. (It is unclear whether the quantitative difference between the theoretical and experimental [100] masses is due entirely to the l-dependence of η, or partly due to some other mechanism, such as the dependence of GaAs dopant impurity behaviour on substrate orientation [22].)

The trend in m^* is thus observed to be the same for the analytically obtained masses m^{*+}_{1av} (bottom) and m^{*+}_{CR} (top; solid line), for the results of full subband structure calculations [19] (centre; triangles) and for the experimental cyclotron resonance masses (top; circles), with $m^*_{100} > m^*_{311} > m^*_{011} > m^*_{211} > m^*_{111}$ in each case. It is seen that on assuming l-dependence of only the leading (bulk) field-dependent term, in the power series expansion for the $N = 1$ and $N = 2$ Landau level dispersions, the trend in the measured CR masses is accurately reproduced, demonstrating that, despite the complexities of hole Landau level structure, the variation of CR mass with heterostructure growth direction can be qualitatively understood in terms of the anisotropy of bulk bandstructure. More complete analysis, based on explicit calculation of hole Landau level structure, is expected to determine whether or not the discrepancy between theoretical and experimental [100] masses is due entirely to the l-dependence of η and to yield accurate quantitative agreement between theoretical and experimental cyclotron resonance masses with no free parameters [21].

In summary, we have measured the dependence on substrate orientation of the effective mass of holes in GaAs–(Ga, Al)As heterojunctions using cyclotron resonance carried out deep in the ultraquantum limit. A manipulation of the standard four-band Luttinger Hamiltonian has been used to isolate the term dominating the behaviour of the hole ground state and to show that the experimentally observed trend in cyclotron resonance masses can be qualitatively explained in terms of the variation of bulk hole mass with crystallographic direction.

This work is supported by EPSRC (UK), the British Council, the European Community and Monbusho (Japan). Useful discussions with Stephen Hill and Ulf Ekenberg are gratefully acknowledged.

References

[1] Wang J, Beton P H, Mori N, Eaves L, Main P C and Henini M 1995 *Proc. 22nd Int. Conf. on the Physics of Semiconductors (ICPS 22) (Vancouver, 1994)* ed D J Lockwood (Singapore: World Scientific) p 1755

[2] Plaut A S, Singleton J, Nicholas R J, Harley R T, Andrews S R and Foxon C T B 1988 *Phys. Rev.* B **38** 1323

[3] Luttinger J M 1956 *Phys. Rev.* **102** 1030

[4] Fasolino A and Altarelli M 1984 *Two Dimensional Systems, Heterostructures and Superlattices (Springer Series in Solid State Sciences 53)* ed G Bauer, F Kuchar and H Heinrich (Berlin: Springer)

[5] Ancilotto F, Fasolino A and Maan J C 1988 *Phys. Rev.* B **38** 1788

[6] Henini M, Rodgers P J, Crump P A, Gallagher B L and Hill G 1995 *J. Cryst. Growth* **150** 446

[7] Langerak C J G M, Singleton J, van der Wel P J, Perenboom J A A J, Barnes D J, Nicholas R J, Hopkins M A and Foxon C T B 1988 *Phys. Rev.* B **38** 13 133

[8] Knight D J E 1982 *Ordered List of Far Infrared Laser Lines* ISSN 0309-3050 (Teddington, UK: National Physical Laboratory)

[9] Miura N, Nojiri H and Imanaka Y 1995 *Proc. 22nd Int. Conf. on Physics of Semiconductors (ICPS 22) (Vancouver, 1994)* ed D Lockwood (Singapore: World Scientific) p 1111

[10] Hill S, Cole B E, Singleton J, Chamberlain J M, Rodgers P J, Janssen T J B M, Pattenden P A, Gallagher B L, Hill G and Henini M 1995 *Physica* B **211** 440

Cole B E, Hill S O, Imanaka Y, Shimamoto Y, Batty W, Singleton J, Miura N, Chamberlain J M, Henini M and Cheng T 1995 *Proc. 11th Int. Conf. on the Electronic Properties of Two Dimensional Systems (Nottingham, 1995)*; *Surf. Sci.* at press

[11] Cole B E, Hill S O, Imanaka Y, Shimamoto Y, Batty W, Singleton J, Chamberlain J M, Miura N, Henini M and Cheng T 1995 *Phys. Rev.* B at press

[12] Bastard G 1988 *Wave Mechanics Applied to Semiconductor Heterostructures* (Les Ulis: Les Editions de Physique)

[13] Ekenberg U and Altarelli M 1985 *Phys. Rev.* B **32** 3712

[14] A similarity transformation has been performed on the Hamiltonian so that it is always diagonal for $k_{\rho'} = 0$ and no subband mixing occurs at the centre of the two-dimensional Brillouin zone [15]. The corresponding bulk Bloch functions are therefore not the standard $|J, m_J\rangle$ basis.

[15] Goldoni G and Peeters F M 1995 *Phys. Rev.* B in press

[16] We use the term 'quantum well' in a general sense to describe all possible one-dimensional potentials in heterostructures.

[17] O'Reilly E P and Witchlow G P 1986 *Phys. Rev.* B **34** 6030

[18] Shanabrook B V, Glembocki O J, Broido D A and Wang W I 1989 *Superlatt. Microstruct.* **5** 503

[19] Meney A T 1992 *Superlatt. Microstruct.* **11** 387

[20] Foreman B A 1994 *Phys. Rev.* B **49** 1757

[21] Batty W, Cole B E and Chamberlain J M 1995 to be published

[22] Ekenberg U 1987 *Semicond. Sci. Technol.* **2** 802